BRAIN
ORIGINAL ARTICLE

UNC13B variants associated with partial epilepsy with favourable outcome

Jie Wang,[1,2,†] Jing-Da Qiao,[1,2,†] Xiao-Rong Liu,[1,2] De-Tian Liu,[1,2] Yan-Hui Chen,[3] Yi Wu,[3] Yan Sun,[4] Jing Yu,[4] Rong-Na Ren,[5] Zhen Mei,[5] Yu-Xi Liu,[6] Yi-Wu Shi,[1,2] Mi Jiang,[1,2] Si-Mei Lin,[1,2] Na He,[1,2] Bin Li,[1,2] Wen-Jun Bian,[1,2] Bing-Mei Li,[1,2] Yong-Hong Yi,[1,2] Tao Su,[1,2] Han-Kui Liu,[7] Wei-Yue Gu[8] and Wei-Ping Liao[1,2] for the China Epilepsy Gene 1.0 Project

[†]These authors contributed equally to this work.

The unc-13 homolog B (*UNC13B*) gene encodes a presynaptic protein, mammalian uncoordinated 13-2 (Munc13-2), which is highly expressed in the brain—predominantly in the cerebral cortex—and plays an essential role in synaptic vesicle priming and fusion, potentially affecting neuronal excitability. However, the functional significance of the *UNC13B* mutation in human disease is not known.

In this study, we screened for novel genetic variants in a cohort of 446 unrelated cases (families) with partial epilepsy without acquired causes by trio-based whole-exome sequencing.

UNC13B variants were identified in 12 individuals affected by partial epilepsy and/or febrile seizures from eight unrelated families. The eight probands all had focal seizures and focal discharges in EEG recordings, including two patients who experienced frequent daily seizures and one who showed abnormalities in the hippocampus by brain MRI; however, all of the patients showed a favourable outcome without intellectual or developmental abnormalities. The identified *UNC13B* variants included one nonsense variant, two variants at or around a splice site, one compound heterozygous missense variant and four missense variants that cosegregated in the families. The frequency of *UNC13B* variants identified in the present study was significantly higher than that in a control cohort of Han Chinese and controls of the East Asian and all populations in the Genome Aggregation Database (gnomAD). Computational modelling, including hydrogen bond and docking analyses, suggested that the variants lead to functional impairment. In *Drosophila*, seizure rate and duration were increased by *Unc13b* knockdown compared to wild-type flies, but these effects were less pronounced than in sodium voltage-gated channel alpha subunit 1 (*Scn1a*) knockdown *Drosophila*. Electrophysiological recordings showed that excitatory neurons in *Unc13b*-deficient flies exhibited increased excitability.

These results indicate that *UNC13B* is potentially associated with epilepsy. The frequent daily seizures and hippocampal abnormalities but ultimately favourable outcome under anti-epileptic therapy in our patients indicate that partial epilepsy caused by *UNC13B* variant is a clinically manageable condition.

1 Institute of Neuroscience and Department of Neurology of the Second Affiliated Hospital of Guangzhou Medical University, Guangzhou 510260, China
2 Key Laboratory of Neurogenetics and Channelopathies of Guangdong Province and the Ministry of Education of China, Guangzhou 510260, China
3 Department of Pediatrics, Fujian Medical University Union Hospital, Fujian 350001, China
4 Department of Pediatrics, People's Hospital of Xinjiang Uygur Autonomous Region, Urumqi, Xinjiang 830001, China
5 Department of Pediatrics and Neurosurgery, 900 Hospital of the Joint Logistics Team, Fujian 350025, China

Received January 07, 2021. Revised March 25, 2021. Accepted April 03, 2021. Advance access publication April 20, 2021

6 Department of Neurology, The First Affiliated Hospital of Shanxi Medical University, Shanxi 030001, China
7 Key Laboratory of Diseases and Genomes, BGI-Genomics, BGI-Shenzhen, Shenzhen 518000, China
8 Department of Translational Medicine Center, Chigene (Beijing) Translational Medical Research Center Co., Beijing 100176, China

Correspondence to: Dr Wei-Ping Liao
Institute of Neuroscience, The Second Affiliated Hospital of Guangzhou Medical University
Chang-Gang-Dong Road 250, Guangzhou 510260, China
E-mail: wpliao@163.net

Keywords: UNC13B; loss of function; partial epilepsy; *Drosophila* knockdown model; electrophysiology

Introduction

Partial (focal) epilepsy is a group of common epilepsies with variable aetiologies and outcomes. In some patients, focal epilepsy has an acquired cause such as trauma, infection, immune abnormalities, or neoplasm[1,2]; however, in most cases, the aetiology is unknown. Idiopathic focal epilepsy (IFE), also known as localization-related idiopathic epilepsy (G40.0 in ICD-10 2016, World Health Organization), is a common subtype of focal epilepsy with generally good prognosis; it typically manifests in childhood as benign epilepsy with centrotemporal spikes (BECTS; MIM: 117100), which affects around 0.2% of the population.[3] Around 4.9% of the patients with BECTS harbour a variant of the glutamate ionotropic receptor N-methyl-D-aspartate type subunit 2A (*GRIN2A*) gene.[4] Other possible causative genes of IFE include DEP domain-containing 5, GATOR1 subcomplex subunit (*DEPDC5*), elongator acetyltransferase complex subunit 4 (*ELP4*), leucine-rich glioma inactivated 1 (*LGI1*), and sushi repeat-containing protein X-linked 2 (*SRPX2*), with variants of these genes identified in rare cases.[5–8] However, the genetic causes of IFE are usually undetermined.[9] In this study, we screened for novel genetic variants in a cohort of 446 unrelated cases (families) with partial epilepsy without acquired causes by trio-based whole-exome sequencing (WES). Variants of the unc-13 homolog B (*UNC13B*) gene were identified in eight unrelated families, and we established a *Drosophila* knockdown model to investigate the role of *UNC13B* variant in epilepsy.

Materials and methods

Patients

A total of 446 unrelated cases (trios) were recruited, including 313 consecutive cases at the Epilepsy Centre of The Second Affiliated Hospital of Guangzhou Medical University from 2012 to 2019; and 133 cases from Fujian Medical University Union Hospital, 900 Hospital of the Joint Logistics Team, People's Hospital of Xinjiang Uygur Autonomous Region, and The First Affiliated Hospital of Shanxi Medical University in 2019. Detailed clinical information, including seizure onset age, seizure type and frequency, course of seizure, response to anti-epileptic treatment, family history and findings from general and neurological examinations, was collected. Brain MRI scans were performed to identify abnormalities in brain structure. Video EEGs, including hyperventilation, intermittent photic stimulation and sleep recording, were performed and the results were reviewed by two qualified investigators. Epileptic seizures and epilepsy syndromes were diagnosed and classified according to Commission on Classification and Terminology of the International League Against Epilepsy criteria (1989, 2001, 2010 and 2017). All enrolled patients were diagnosed with epilepsy that was characterized by focal seizures or focally originating secondary generalized tonic-clonic seizures. In all cases, EEG recordings showed focal discharges with features of idiopathic epilepsy including shifting, bilateral or multiple focal discharges with normal background. Participants with acquired causes or typical generalized seizures, such as absence, atonic and generalized myoclonic seizures, were excluded. All participants were Han Chinese with four Han Chinese grandparents, and were born to non-consanguineous Chinese parents. In 98 cases, there was a family history of epilepsy or febrile seizures. All enrolled patients were followed up for at least 1 year at epilepsy centres. As a control group, we recruited 150 patients with idiopathic generalized epilepsy. Additionally, WES was performed in 296 healthy Chinese volunteers who served as a normal control group as in our previous report.[10] We also analysed a Han Chinese control population ($n = 10\,640$) from a recent large-scale low-depth whole-genome sequencing study on major depressive disorder (we previously obtained the original data through the two provided links),[11] and compared the frequencies of the identified variants with those in the control participants of the East Asian and all populations in the Genome Aggregation Database (gnomAD). This study was approved by the ethics committee of The Second Affiliated Hospital of Guangzhou Medical University, and written, informed consent was obtained from all patients and their parents.

Whole-exome sequencing and genetic analysis

Blood samples were obtained from the probands, their parents and available family members to determine the origin of the identified genetic variants. Genomic DNA was extracted from the blood samples using the FlexiGene DNA kit (Qiagen). Trio-based WES was performed on a HiSeq 2000 system (Illumina) as previously reported.[10,12,13] The sequencing data were generated by massive parallel sequencing with >125 times average depth and >98% coverage in the capture region of the chip to obtain high-quality reads that were mapped to the Genome Reference Consortium Human Genome build 37 (GRCh37) by Burrows–Wheeler alignment. Single-nucleotide point variants and indels were called with the Genome Analysis Toolkit. To identify candidate causative variants in each trio, we adopted a case-by-case analytical approach. We first prioritized the rare variants with a minor allele frequency <0.005 in the 1000 Genomes Project, Exome Aggregation Consortium and gnomAD. We retained potentially pathogenic variants containing frameshift, nonsense, canonical splice site, initiation codon and missense mutations predicted as being damaging using *in silico* tools (http://varcards.biols.ac.cn/). Finally, we screened for possibly disease-causing mutations/variants in each case under five different models: (i) epilepsy-associated gene; (ii) *de novo* variant dominant; (iii) autosomal recessive inheritance, including homozygous and compound heterozygous variants; (iv) X-linked; and (v) cosegregation analysis. To identify novel epilepsy-associated genes, we set aside the known epilepsy-associated genes,[14] and selected the genes with null variants, *de novo* variants, bi-allelic variants, hemizygous variants and variants with

segregations for further studies to define the gene-disease association. The candidate variants were validated by Sanger sequencing. All *UNC13B* variants identified in this study were annotated to reference transcript NM_006377.3.

Computational modelling and docking

The structure of mammalian uncoordinated 13-2 (Munc13-2), the protein encoded by *UNC13B*, was modelled using SWISS-MODEL (https://swissmodel.expasy.org/) to predict the effect of missense variants on protein structure. The model of the Thr103Met variant was based on the 2cjs.1.pdb template and those of the Arg661Cys, Gly794Asp and Gly882Trp variants were based on the 5ue8.1.pdb template in the Protein Data Bank (PDB) (https://www.rcsb.org/). Hydrogen bonding was analysed and visualized using PyMOL v.2.3 software (https://pymol.org/2/). After computational modelling, the docking of Arg661Cys, Gly794Asp and Gly882Trp with calmodulin (PDB: 2o60) was predicted using ZDOCK (http://zdock.umassmed.edu/). The interaction of the calmodulin-binding domain of neuronal nitric oxide synthase with wild-type or mutant Munc13-2 was analysed. The docking results were visualized using PDBePISA (https://www.ebi.ac.uk/pdbe/pisa/).

Fly stocks

Flies were fed standard cornmeal and maintained in incubator at 25°C (except where otherwise noted) and 60–70% humidity on a 12:12-h light/dark cycle. *UAS-Unc13b-RNAi* (THU2483/FBst0029548), *UAS-Scn1a-RNAi* (*para-RNAi*, positive control) and *UAS-Chd3-RNAi* (negative control) flies were donated by Tsing Hua Fly Center (Tsinghua University, Beijing, China). The green fluorescent protein (GFP) reporter line *UAS-EGFP* and a double balancer line were purchased from Bloomington Fly Stock Center. The Gal4 driver line *tub-Gal4* was a gift from Professor Liu Ji-Yong (Guangzhou Medical University, Guangzhou, China), and the *UAS-mCD8::GFP* line was a gift from Professor KE Ya (The Chinese University of Hong Kong, Hong Kong). *Canton-S* was used as the wild-type line in this study.

Seizure behaviour test

The *tub-Gal4* line was crossed with *Unc13b-RNAi* to establish global *Unc13b* knockdown flies (*tub-Gal4 > Unc13b-RNAi*).[15] The bang-sensitive (BS) test was performed on flies 3–5 days after eclosion and seizure-like behaviour was assessed.[16] Flies were anaesthetized with CO_2 and transferred to new clean food vials 1 day before testing. About two to five flies were placed in one vial and mechanically stimulated with a vortex mixer (VWR) at maximum speed for 10 s. The percentage and duration of BS paralysis in flies were recorded.

Electrophysiology and morphological analysis

Attached recording was performed in *Unc13b* knockdown flies using an established electrophysiological method.[17] Fly brains were dissected as previously described[18] and transferred to a recording chamber with fly external solution and immobilized with a C-sharp holder. The standard external solution contained (in mM) 101 NaCl, 1 $CaCl_2$, 4 $MgCl_2$, 3 KCl, 5 glucose, 1.25 NaH_2PO_4 and 20.7 $NaHCO_3$ (pH 7.2 and 250 mOsm). All dissection procedures were performed under a dissecting microscope. The anterior side of the brain was positioned facing upwards to enable observation of the soma of projection neurons on the brain surface. A patch pipette filled with external solution was used for attached recording with a 700B amplifier. Data were acquired with a Digidata 1440B digital–analogue converter (Molecular Devices) and pClamp v.10.5 software (Molecular Devices).

To examine morphologic alterations in the brain, *UAS-mCD8::GFP* was used to generate *tub-Gal4 > UAS-mCD8::GFP/UAS-Unc13b-RNAi and tub-Gal4 > UAS-mCD8::GFP* lines of *Unc13b* knockdown and control flies, respectively, that were labelled with GFP. The brain was dissected and fixed with 4% paraformaldehyde in PBS with 0.1% Triton™ X-100 for 1 h at 25°C, then washed and permeabilized three times with 0.3% Triton™ X-100 PBS. Images were captured using a confocal microscope (SP8; Zeiss) and analysed with ImageJ software (National Institutes of Health, Bethesda, MD, USA).

Statistical analysis

All quantitative data are presented as mean ± standard error of the mean (SEM). The Student's *t*-test was used to compare two independent or paired samples. One-way ANOVA was used to compare multiple samples, and Tukey's *post hoc* test was used to evaluate differences between two groups. The Kruskal–Wallis test was used to assess non-parametric data, and a two-tailed Fisher's exact test was used to compare allele frequencies between groups. Statistical analyses were performed with GraphPad Prism 7.00 and SPSS 20. The cut-off value for statistical significance was 0.05.

Data availability

Raw data were generated at Institute of Neuroscience, The Second Affiliated Hospital of Guangzhou Medical University. Derived data supporting the findings of this study are available from the corresponding author on request.

Results

Identification of *UNC13B* variants

Variants in *UNC13B* were identified in eight unrelated patients with partial epilepsy, including one nonsense variant (c.135G > A/p.Trp45X), two variants at or around a splice site (c.4008+1G > T and c.4330+7G > A) and six missense variants (c.308C > T/p.Thr103Met, c.662G > A/p.Arg221Gln, c.1190C > T/p.Ser397Phe, c.1981C > T/p.Arg661Cys, c.2381G > A/p.Gly794Asp and c.2644G > T/p.Gly882Trp). Two of the missense variants, c.308C > T/p.Thr103Met and c.1190C > T/p.Ser397Phe, constituted a pair of compound heterozygous variants. The variants c.135G > A/p.Trp45X and c.4330+7G > A were *de novo*. The c.4008+1G > T variant was from an unaffected mother. Except for the compound heterozygous variants, the other four heterozygous missense variants were identified in families with more than one affected individual (Fig. 1).

The c.135G > A/p.Trp45X variant was potentially deleterious, yielding a truncated transcript that gave rise to a non-functional Munc13-2 protein or haploinsufficiency. The c.4008+1G > T variant disrupted the original splice donor site and was predicted to introduce a cryptic splice donor site in exon 34 that resulted in the skipping of the exon or deletion of its last nucleotide with consequent translational frameshift. Although the functional outcome is unknown, c.4330+7G > A was a *de novo* variant that was not listed in any public databases (including 1000 Genomes Project, Exome Sequencing Project and gnomAD). Three other variants (c.135G > A/p.Trp45X, c.2381G > A/p.Gly794Asp, and c.2644G > T/p.Gly882Trp) were also not found in gnomAD. The other five variants were present at an extremely low frequency in gnomAD (controls of all populations and East Asian populations; see Supplementary Tables 1 and 2). These variants were not observed in our 296 normal control participants except for c.1190C > T/p.Ser397Phe, which was present in one individual. The c.1190C > T/p.Ser397Phe variant was one of the pair of

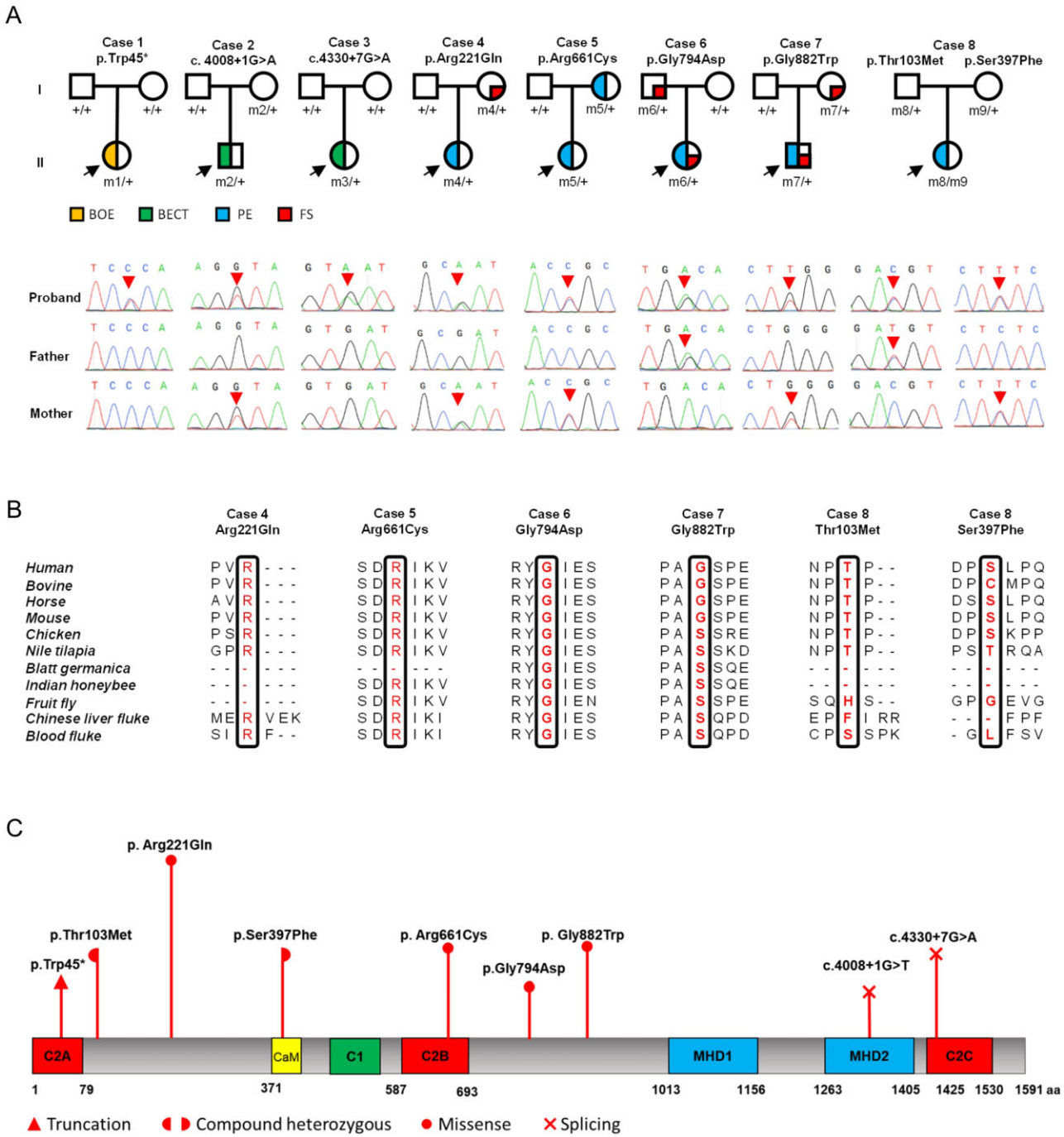

Figure 1 Genetic data of cases with *UNC13B* variants. (**A**) Pedigrees and DNA sequencing chromatogram of the eight cases with *UNC13B* variants and their corresponding phenotypes. (**B**) Amino acid sequence alignment of the six missense variants with protein substitutions show that Arg221, Arg661 and Gly794 are highly conserved across species. Thr103 and Gly882 are highly conserved in vertebrates but less conserved in lower animals, while Ser397 shows a low degree of conservation. (**C**) Schematic illustration of the Munc13-2 protein and the location of the *UNC13B* variants or protein substitutions identified in this study.

compound heterozygous variants in *UNC13B* (the other being c.308C>T/p.Thr103Met).

We performed a comparative analysis on the frequencies of the variant *UNC13B* alleles in the present cohort and control populations in gnomAD. Nine mutant alleles in a total of 892 (446 cases) were detected in our cohort, which were present at frequencies of 0.00199 (18/9042) in the controls of the East Asian population and 0.00027 (29/109 378) in the controls of all populations in gnomAD. The differences in frequencies of the identified variants between our cohort and the two control populations in gnomAD were statistically significant (9/892 versus 18/9042, $P = 4.08 \times 10^{-4}$; 9/892 versus 29/109378, $P = 2.05 \times 10^{-11}$, respectively). Except for c.2644G>T/p.Gly882Trp, these variants were absent in the cohort of 10 640 Han Chinese in the study on major depressive disorder[11] (9/892 versus 1/21280, $P = 2.79 \times 10^{-12}$) (Supplementary Table 2).

None of the 12 affected individuals had pathogenic or likely pathogenic variants in the 977 genes known to be associated with epileptic phenotypes.[14] In control patients with idiopathic

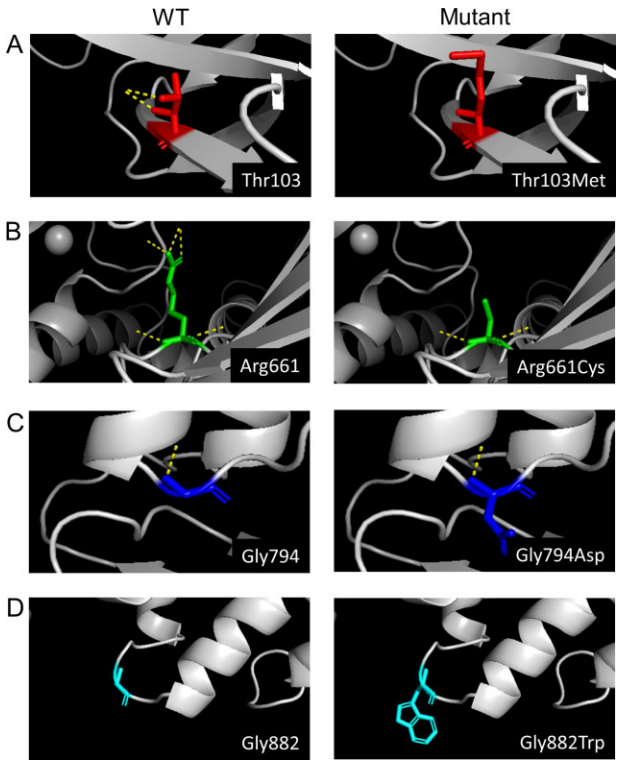

Figure 2 Schematic illustration of hydrogen bonds in Munc13-2. (**A**) *Left*: Thr103 (red) forms two hydrogen bonds (yellow) with Gly102. *Right*: Thr103Met destroys the two hydrogen bonds. (**B**) *Left*: Arg661 (green) forms five hydrogen bonds (yellow)—one each with Tyr492, Ser659 and Lys663 and two with Glu493. *Right*: Arg661Cys destroys three of the five hydrogen bonds without affecting those with Ser659 and Lys663. (**C**) *Left*: Gly794 (blue) forms one hydrogen bond (yellow) with Ala790. *Right*: Gly794Asp does not affect hydrogen bonding in Munc13-2. (**D**) Gly882 (cyan) does not form hydrogen bonds with any other residue, and Gly882Trp does not affect hydrogen bonding in Munc13-2.

generalized epilepsy, we did not find any deleterious, *de novo* or compound heterozygous *UNC13B* variants or cosegregating variants.

The missense variants were predicted to be damaging by more than one of the commonly used *in silico* prediction tools (Supplementary Table 1). Protein sequence alignment indicated that Arg221Gln, Arg661Cys and Gly794Asp were located at residues that are highly conserved across species; Thr103 and Gly882 are highly conserved in vertebrates but less so in lower animals (Fig. 1B). The Ser397Phe was located at a less conserved site but was predicted to be conserved by *in silico* tools (Supplementary Table 1).

Munc13-2 is a large protein with seven evolutionarily conserved domains including an N-terminal C2 domain (C2A), Ca^{2+}/phospholipid-binding C2 domain (C2B), C-terminal non–Ca^{2+}-binding C2 domain (C2C), calmodulin-binding domain (CaM), phorbol ester/diacylglycerol-binding C1 domain (C1) and two Munc13 homology domains (MHD1 and MHD2) (Fig. 1C).[19] Ser397Phe and Arg661Cys were located in the CaM and C2B domains, respectively, which are regulated by Ca^{2+} and mediate neurotransmission and neural plasticity. Alterations in hydrogen bonding caused by Thr103Met, Arg661Cys, Gly794Asp and Gly882Trp were analysed using available templates in SWISS-MODEL and PyMOL (Fig. 2). Thr103 formed two hydrogen bonds with Glu102 that were destroyed by Thr103Met (Fig. 2A). Gly661 formed five hydrogen bonds with Tyr492, Glu493, Ser659 and Lys663; Arg661Cys destroyed the bond with Tyr492 and the two with Glu493, leaving two hydrogen bonds with Ser659 and Lys663 (Fig. 2B). The Gly794Asp and Gly882Trp did not significantly affect hydrogen bonding (Fig. 2C and D). The Arg661Cys, Gly794Asp and Gly882Trp were located in a region between C2B and MHD1; Gly794Asp potentially altered the docking site in the calmodulin–Munc13-2 complex, with a significantly decreased interface area (from 1004.5 to 610.6 $Å^2$) and Gibbs free energy (Δ^iG from 14.6 to −10.1 kcal/mol) (Fig. 3A and C). The Arg661Cys and Gly882Trp did not have any significant effects on docking (Fig. 3B and D).

Clinical features

UNC13B variants were identified in eight cases (families) with 12 affected individuals (Fig. 1 and Table 1). The eight probands all had focal seizures or focally originating tonic-clonic seizures; all had focal discharges in EEG recordings. Two probands were diagnosed as BECTS and one as benign occipital epilepsy. The other five

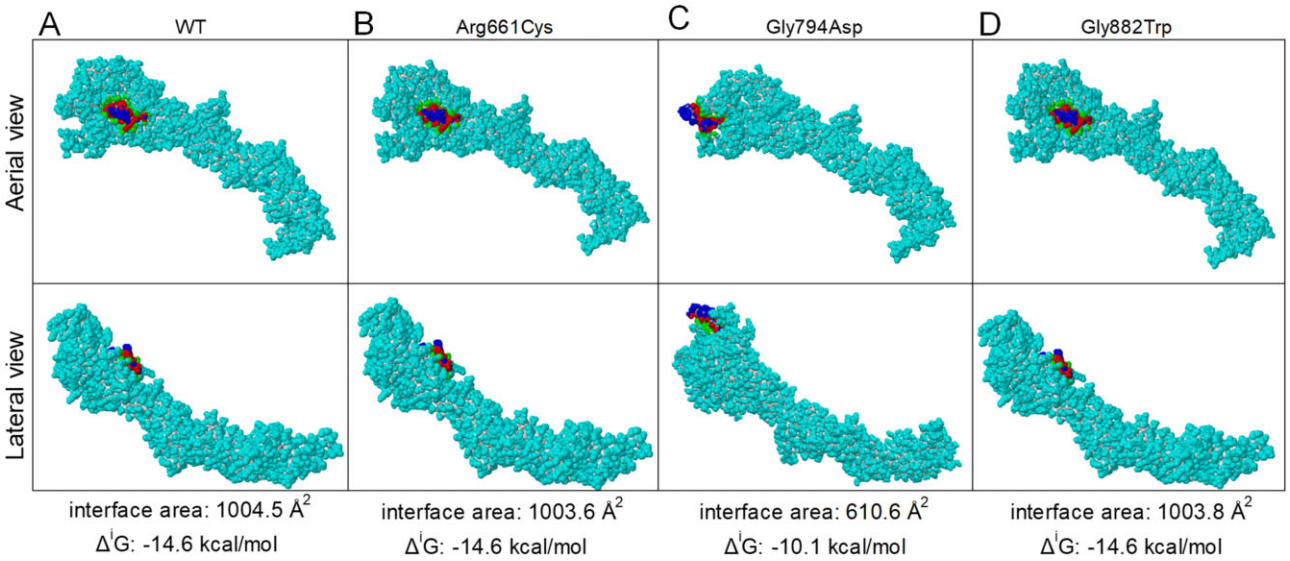

Figure 3 Model of calmodulin docking on Munc13-2 and the effect of variants. (**A**) Complex of wild-type (WT) Munc13-2 and calmodulin. (**B–D**) Complex of mutant Munc13-2 and calmodulin. (**C**) Gly794Asp alters the docking site, interface area and Gibbs free energy of Munc13-2.

Table 1 Clinical features of individuals with *UNC13B* variants

Case ID	Variant (NM_006377.3)	Sex	Age, years	Seizure onset	Seizure course	Seizure timing	Seizure-free duration, years	Effective AED	EEG	Brain MRI	Development	Diagnosis
1	c.135G>A (p.Trp45X)	Female	17	7 y	sGTCS and CPS, 1/mo for 1 y	Nocturnal	9 y	OXC	Left occipital spikes and slow spike waves	Normal	Normal	BOE
2	c.4008+1G>T	Male	10	5 y	GTCS, 1–2/mo for 3 y	Mostly nocturnal	2 y	VPA, LEV	Right central-temporal sharp and sharp-slow waves	NA	Normal	BECTS
3	c.4330+7G>A	Male	17	12 y	sGTCS, 1–3/mo for 8 mo	Nocturnal	4 y	OXC	Left, right and bilateral central-temporal spikes	Normal	Normal	BECTS
4–1	c.662G>A (p.Arg221Gln)	Female	2	3 mo	CPS, 10–15/d for 1 mo	Mostly on awakening	2 y	OXC	Ictal: right frontal-originating CPS; interictal: no discharge	Normal	Normal	PE
4–2		Female	34	1 y	FS, 2–3 for 1 y	–	32 y	–	NA	Normal	Normal	FS
5–1	c.1981C>T (p.Arg661Cys)	Female	4	8 mo	sGTCS and CPS, 1–2/wk for 4 mo	Mostly diurnal	3 y	LEV	Frontal and midline sharp waves and sharp-slow waves	Normal	Normal	PE
5–2		Female	32	3 y	GTCS in childhood, occasionally in adulthood	NA	4 y	–	NA	Normal	Normal	UE
6–1	c.2381G>A (p.Gly794Asp)	Female	19	7 mo	FS once at 7 mo, GTCS and CPS 2–4/y from age 14–18 y	Game-precipitated, nocturnal	1 y	LTG, VPA	Left central-temporal small spikes	Normal	Normal	FS, PE
6–2		Male	40	1 yr	FS twice	–	39 y	–	NA	Normal	Normal	FS
7–1	c.2644G>T (p.Gly882Trp)	Male	7	2 yr	FS and afebrile seizures 4–5/y for 2 y	Diurnal and Nocturnal	3 y	LEV	Right frontal and central-temporal spikes and sharp waves, and sharp/slow spike waves	Normal	Normal	FS, PE
7–2		Female	30	2 yr	FS 1–2/y for 2 y	–	26 y	–	NA	Normal	Normal	FS
8	c.308C>T (p.Thr103Met) c.1190C>T (p.Ser397Phe)	Female	29	22 yr	sGTCS and CPS, 2–3/mo and up to 5/day for 6 y	Diurnal and nocturnal	1 y	LTG	Ictal: 1 sGTCS and 4 CPS of indeterminate origin; interictal: left and right temporal spikes and sharp waves	Abnormal (Fig. 4E and F)	Normal	PE

AED = anti-epileptic drug; BECTS = benign childhood epilepsy with centrotemporal spikes; BOE = benign occipital epilepsy; CPS = complex partial seizure; FS = febrile seizure; GTCS = generalized tonic-clonic seizure; LEV = levetiracetam; LTG = lamotrigine; mo = months; NA = not available; OXC = oxcarbazepine; PE = partial epilepsy; sGTCS = secondary generalized tonic-clonic seizure; UE = unclassified epilepsy; VPA = valproate; wk = week; y = years.

probands were diagnosed as partial epilepsy, including two with antecedent febrile seizures. In the eight families, no any other members except the parents have a history of epilepsy or febrile seizures. Interictal or ictal epileptic discharges were detected in all of the probands. The interictal discharges in seven patients showed focal abnormalities with features of idiopathic epilepsies including shifting, bilateral, multiple focal discharges with normal backgrounds or trends of generalization especially during sleep (Fig. 4); no photosensitivity were recorded in these patients. Frequent daily seizures occurred in two patients (Cases 4-1 and 8; Table 1), but no any prolonged seizures or status epilepticus were observed in the affected individuals. All patients were seizure-free after anti-epileptic treatment. The patient with a compound heterozygous variant had secondary generalized tonic-clonic seizures or complex partial seizures at a frequency of up to five times per day (five seizures recorded during one night). The condition lasted for 6 years, which was longer than in other cases. The patient's brain MRI showed structural asymmetry between the right and left hippocampi; the right hippocampus was smaller and had a slightly higher signal, and the left hippocampus had an indistinct boundary with surrounding tissues (Fig. 4E and F). The patient did not initially respond to valproate (25 mg/kg/day) and levetiracetam (25 mg/kg/day), but achieved seizure freedom after 1 year of lamotrigine monotherapy (150 mg/day). All affected individuals did not experience with ketogenic diet or vagus nerve stimulation therapy. The seizure onset age of the 12 affected individuals ranged from 3 months to 22 years old, with a median age of onset of 2 years. Five had febrile seizures, and none had intellectual or developmental abnormalities.

The eight cases with *UNC13B* variants showed several common features: (i) partial epilepsy with EEG features of idiopathic epilepsy, including shifting, bilateral or multiple focal discharges with normal background or trends of generalization especially during sleep; (ii) no intellectual or developmental abnormalities; (iii) favourable outcome, even in the two patients experienced frequent daily seizures and the patient with abnormalities in the hippocampus shown by brain MRI; (iv) familial history of epilepsy or febrile seizures in half of the cases; and (v) the frequent daily seizures without neurological consequences appeared to be different from the patients with common partial epilepsies.

Unc13b knockdown in flies

To clarify the relationship between *UNC13B* variant and seizure sensitivity, we examined BS seizure-like behaviour in *tub-Gal4 > Unc13b-RNAi Unc13b* knockdown flies. Interestingly, *Unc13b* knockdown was pre-adult lethal. There were no adults among the *tub-Gal4 > Unc13b-RNAi* flies treated at 25°C in the pre-adult stage, indicating that *Unc13b* plays a critical role in the early life of flies. Temporally controlled knockdown was performed to evaluate the effect of *Unc13b* deficiency on epileptogenesis. The *tub-Gal4 > Unc13b-RNAi* flies were maintained at 18°C until eclosion, as RNAi efficiency declined at the pre-adult stage. Adult flies were collected and maintained at 29°C for 48 h to increase gene knockdown efficiency before behavioural testing. The *tub-Gal4 > Unc13b-RNAi* flies exhibited the typical seizure-like behaviour observed in other seizure mutants (*bss*, *tko* and *para* mutants).[20] The three phases of seizure activity in the BS test were observed—namely, seizure, paralysis and recovery (Fig. 5A and Supplementary Video 1). About 24.8% of *tub-Gal4 > Unc13b-RNAi* flies showed obvious seizure-like behaviour, which was higher than the rate in *Unc13b-RNAi* control flies [24.83 ± 5.06% ($n = 6$) versus 4.36 ± 1.29% ($n = 7$); $P = 0.008$; Fig. 5B]. The *tub-Gal4 > Scn1a-RNAi* positive control flies had a higher rate of seizures than *tub-Gal4 > Unc13b-RNAi* flies [48.88 ± 2.60% ($n = 5$) versus 24.83 ± 5.06% ($n = 6$); $P = 0.006$]. Most *tub-Gal4 > Unc13b-RNAi* flies recovered within 1–6 s whereas most controls recovered within 0–1 s. In contrast, the recovery time of *tub-Gal4 > Scn1a-RNAi* flies was 3–12 s, which was longer than for *tub-Gal4 > Unc13b-RNAi* flies (Fig. 5C).

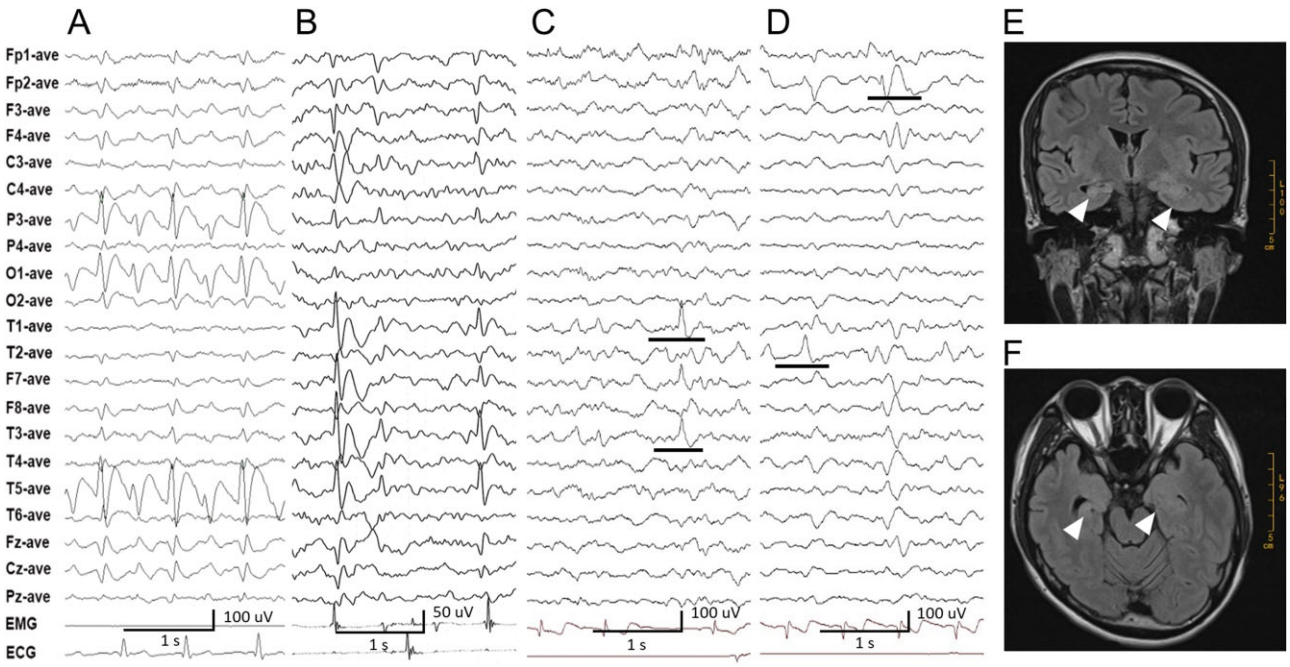

Figure 4 Representative EEG recordings and MRI from patients with *UNC13B* variants. (**A**) Interictal EEG in Case 1 showed left occipital slow spike waves. (**B**) Interictal EEG in Case 3 showed left central-temporal slow spike waves. (**C** and **D**) Interictal EEG in Case 8 showed spikes or sharp waves in the left or right temporal lobe, or of slow spike waves in the right frontal lobe. (**E** and **F**) Coronal and axial T_2-FLAIR MRI of Case 8 revealed structural asymmetry in the hippocampus; the right hippocampus was smaller than the left one, with a slightly higher signal. The boundary between the left hippocampus and surrounding tissues was indistinct.

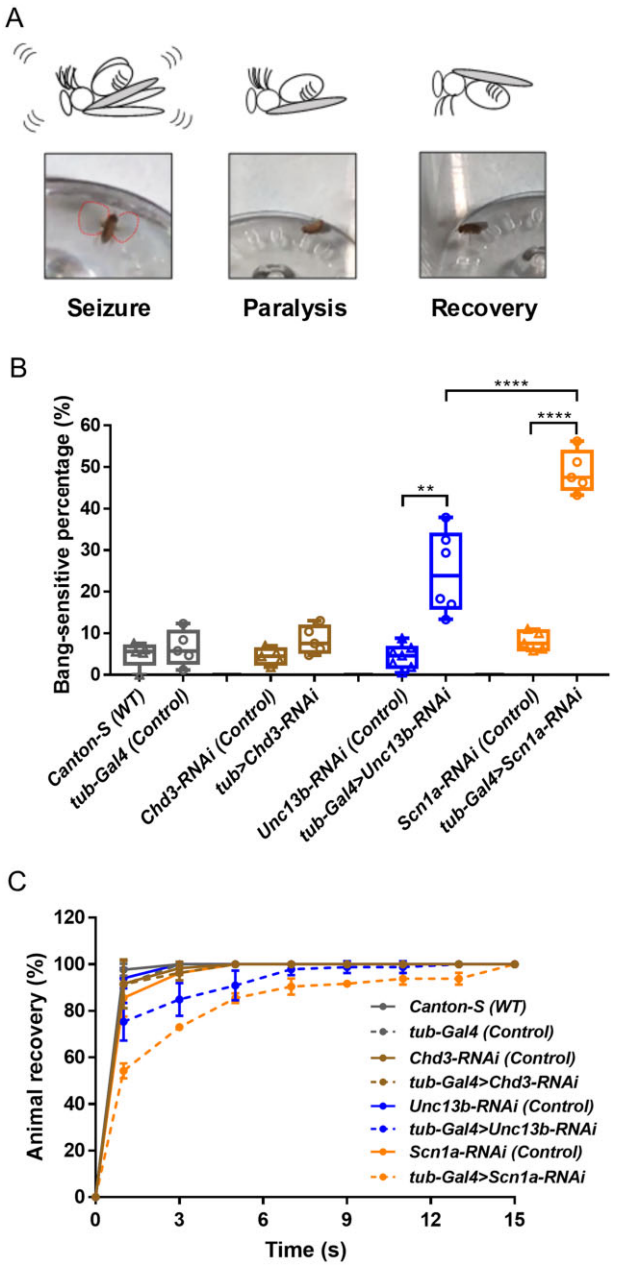

Figure 5 Knockdown of *Unc13b* induces seizure-like behaviour in *Drosophila*. (**A**) Behaviour in the BS paralysis test; the three stages observed in *Unc13b* knockdown flies were seizure (manifesting as vibrating wings, circled in red), paralysis and recovery. (**B**) Seizures occurred at a higher rate in *Unc13b* knockdown flies (*tub-Gal4>Unc13b-RNAi*) than in wild-type (WT) flies (*Canton-S*) and *tub-Gal4>Chd3-RNAi* and other control groups. The *tub-Gal4>Scn1a-RNAi* positive controls had a higher rate of seizures than the *tub-Gal4>Unc13b-RNAi* group. (**C**) The recovery time from seizure was longer in *tub-Gal4>Unc13b-RNAi* than in *Canton-S* but shorter than in *tub-Gal4>Scn1a-RNAi*.

We examined the effect of *Unc13b* deficiency on the electrophysiological activity of projection neurons, which are important excitatory neurons in the central nervous system of *Drosophila*,[21] by attached recording. Extracellular activity (action currents) was detected by loose patching; the membrane resistance was 200–250 MΩ. Typical traces of extracellular action currents of wild-type flies are shown in Fig. 6A. The projection neurons of *Unc13b* knockdown flies (*tub-Gal4>Unc13b-RNAi*) showed a regular burst firing pattern (Fig. 6B). Meanwhile, *tub-Gal4>Unc13b-RNAi* flies had

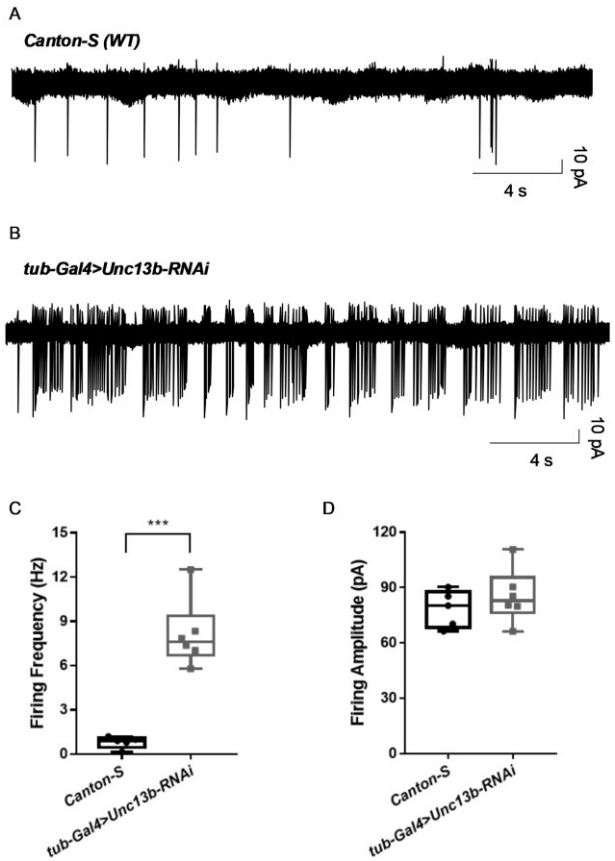

Figure 6 *Unc13b* knockdown induces increased neural excitability in projection neurons. (**A**) Representative trace of extracellular electrical activity in *Canton-S* wild-type (WT) projection neurons showing sporadic action currents. (**B**) Regular high-frequency burst firing was recorded in projection neurons of *tub-Gal4>Unc13b-RNAi* flies. (**C**) Action current frequency was significantly higher in *tub-Gal4>Unc13b-RNAi* than in *Canton-S*. (**D**) There was no difference in amplitude of action currents between *tub-Gal4>Unc13b-RNAi* and *Canton-S*.

significantly higher frequency of extracellular action currents in projection neurons than wild-type flies [8.14 ± 0.94 Hz ($n = 6$) versus 0.76 ± 0.22 Hz ($n = 5$); $P = 0.0003$] (Fig. 6C). There was no significant difference in action current amplitude between *tub-Gal4>Unc13b-RNAi* and wild-type flies [86.65 ± 7.24 pA ($n = 6$) versus 76.80 ± 5.35 pA ($n = 5$); $P = 0.33$] (Fig. 6D).

We examined possible morphological changes in *Unc13b* knockdown flies based on GFP expression. The confocal images showed that *Unc13b* knockdown did not affect the main brain structures (Fig. 7A–F), except for slight loss of the calyx structure that is a part of mushroom body (Fig. 7G and H). As possible abnormalities in the hippocampus were observed in one of the patients (Case 8), we examined the morphology of neurons in the mushroom body, which is considered to be analogous to the mammalian hippocampus, but found that it did not differ between *Unc13b* knockdown and wild-type flies except for slight blurring of the membrane and irregular cell body shape in the mutants (Fig. 7I and J).

Discussion

The *UNC13B* gene is located at chromosomal locus 9p13.3 and spans approximately 243 kb of genomic DNA. Eleven *UNC13B* transcript variants have been described. Isoform 1 (NM_006377.3) composed of 39 exons encodes the 1591-amino acid presynaptic protein Munc13-2, which contains a CaM domain, C1 domain, two

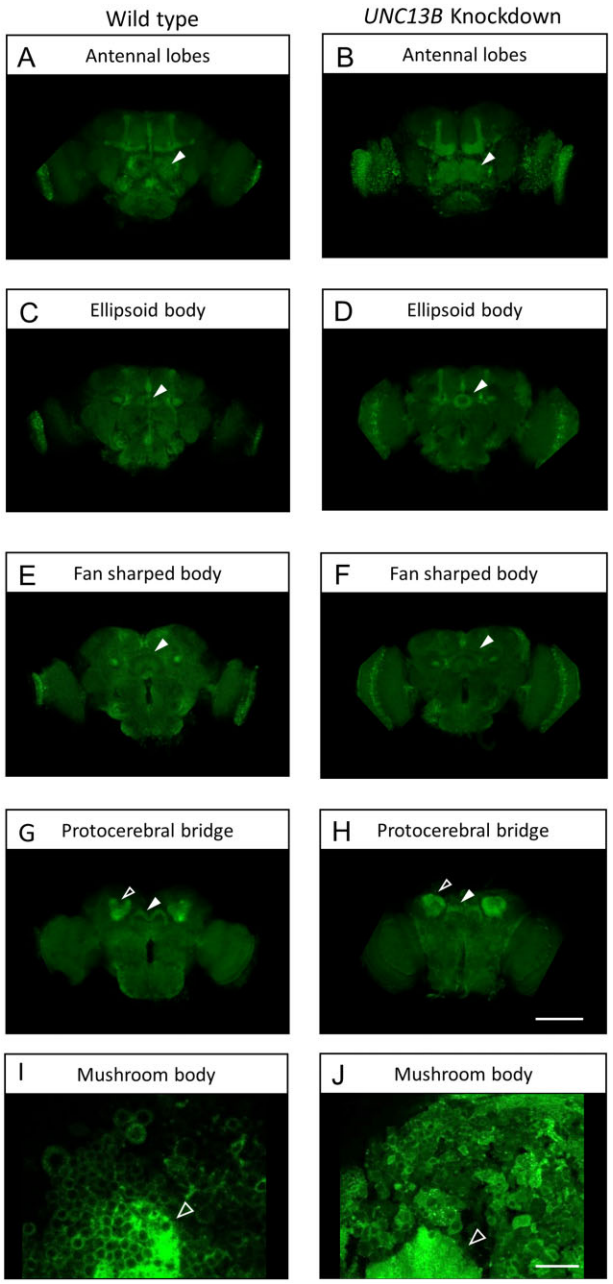

Figure 7 Brain morphology in *Unc13b* knockdown flies. (**A**, **C**, **E** and **G**) Serial images of the brain of a wild-type fly from anterior to posterior showing the structure of antennal lobes (**A**), ellipsoid body (**C**), fan-shaped body (**E**), and protocerebral bridge (filled arrowhead) and mushroom body calyx (open arrowhead) (**G**). (**B**, **D**, **F** and **H**) Serial images of the brain of a *Unc13b* knockdown fly from anterior to posterior showing the structure of antennal lobes (**B**), ellipsoid body (**D**), fan-shaped body (**F**), and protocerebral bridge (white arrowhead) and mushroom body calyx (open arrowhead) (**H**). Scale bar = 100 μm. (**I**) Cell body of neurons (open arrowhead) in the mushroom body of a wild-type fly. (**J**) Cell body of neurons (open arrowhead) in the mushroom body of a *Unc13b* knockdown fly. Scale bar = 10 μm.

Munc13-homology domains and three C2 domains.[22,23] Munc13 along with Munc18 functions in vesicle priming and regulates a readily releasable pool of fusion-competent synaptic vesicles by protecting the soluble N-ethylmaleimide–sensitive factor attachment protein receptor (SNARE) complex, which is essential for synaptic vesicle fusion and may modulate neuroexcitability[24] (Supplementary Fig. 1). The syntaxin-binding protein 1 (*STXBP1*) gene encoding Munc18-1 is associated with epileptic encephalopathy (EIEE-4, MIM: 612164). However, the association between *UNC13B* gene variants and human disease has not been previously reported. Homozygous *UNC13B* knockout mice exhibit abnormal synapse morphology and sporadic seizures (www.informatics.jax.org/marker/MGI:1342278), and specific knockdown of *UNC13B* in the medial prefrontal cortex resulted in neural hyperexcitability in the basolateral amygdala.[25] In the present study, we identified *UNC13B* variants in 12 individuals affected by partial epilepsies and/or febrile seizures from eight unrelated families. The variants included two *de novo* variants, one compound heterozygous variant and four missense variants that co-segregated in the families. The frequency of *UNC13B* variants identified in the present study was significantly higher than that in the control cohort of Han Chinese and controls of the East Asian and all populations in gnomAD. In experiments with *Drosophila*, seizure-like behaviour and increased firing of neurons were observed in *Unc13b* knockdown flies. These findings provide evidence that *UNC13B* is potentially associated with epilepsy.

Variants identified in the present study included a truncating variant, splice-site variant and compound heterozygous variant, suggesting that they are associated with a loss of function. Among the six missense variants with protein substitution, Thr103Met abolished hydrogen bonding with Glu102. Arg221Gln was the most highly conserved residue in the protein sequence alignments. Ser397Phe and Arg661Cys were located in the CaM and C2B domains, respectively. Previous studies have shown that mutations in these domains may affect Ca^{2+} binding and Ca^{2+}-dependent neurotransmitter release.[26,27] Gly794Asp and Gly882Trp were located in an area close to the C2B-MHD1 linker, which is associated with C2B inhibition[28,29]; moreover, Gly794Asp may affect calmodulin docking. In the present study, *Unc13b* knockdown flies showed seizure-like behaviour and increased firing of excitatory neurons. This along with previous data from *UNC13B* knockdown and knockout mice suggests that *UNC13B* loss of function plays a role in cortical excitability and epileptogenesis.[25,30] However, other pathogenic mechanisms such as gain of function and toxicity cannot be excluded. In fact, *UNC13B* gain of function is also predicted to promote transmitter release, similar to gain-of-function mutations in the synaptic protein Munc18-1 (encoded by *STXBP1*) that lead to synaptic vesicle exhaustion and epilepsy.[31,32] Indeed, both loss- and gain-of-function mutations in several genes [e.g. *SCN1A*; *CACNA1A* encoding the $Ca_v2.1$ P/Q voltage-dependent calcium channel; and hyperpolarization-activated cyclic nucleotide gated potassium channel 1 (*HCN1*)] were shown to give rise to similar epilepsy phenotypes.[24,33–35] Further studies are needed to clarify the functional consequences of each variant and their contribution to epileptogenesis.

All patients in the present work with *UNC13B* variants had focal seizures and focal discharges that were usually multifocal. We did not find *UNC13B* variants in patients with idiopathic generalized epilepsy. *UNC13B* is predominantly expressed in the cortex,[36] which provides an anatomic basis for the pathogenesis of focal seizures and multifocal EEG discharges. Patients with *UNC13B* variants had favourable outcome without intellectual or developmental abnormalities and all achieved seizure freedom, including the two patients who experienced daily seizures during their illness. Three individuals had only febrile seizures. In experiments with *Drosophila*, the frequency of seizures was lower and their duration was shorter in *Unc13b* knockdown flies compared to *Scn1a*-deficient flies. *SCN1A* is the most common epilepsy gene with more than 1727 identified mutations, mostly in patients with severe Dravet syndrome (www.caae.org.cn/gzneurosci/scn1adatabase/).[37] Our findings in flies are consistent with the relatively mild clinical phenotypes and favourable outcomes of patients with *UNC13B*

variants. Moreover, it was previously reported that normal Munc13 function is required for synaptic secretory activity rather than synaptogenesis in mice.[30]

The patient with a compound heterozygous variant in *UNC13B* presented frequent daily seizures, slight structural abnormalities in the hippocampus, had a longer course of illness and initially responded poorly to treatment, suggesting that biallelic variants lead to a more severe phenotype. On the other hand, three heterozygous *UNC13B* variants (c.4008+1G>T, c.662G>A/p.Arg221Gln and c.1981C>T/p.Arg661Cys) presented a low frequency in control population of gnomAD (Supplementary Table 1). Generally, variants in a gene may differ in damage effect, which varies from mild to severe, depending on factors such as the molecular subregional effect as shown in our recent study.[38] It is possible that the *UNC13B* variants mentioned above were of less damaging effect and were associated with susceptibility or mild epileptic phenotype with incomplete penetrance; or *UNC13B* is a susceptibility gene of epilepsy. Additional genetic studies are required to determine the pathogenic potential of *UNC13B* and establish the extremes of severity of the *UNC13B* mutant phenotype. *De novo UNC13B* variants were previously reported in patients with bipolar disorder and autism spectrum disorder[39–41]; therefore, the association between *UNC13B* variants and neurologic disorders warrants further investigation.

In conclusion, we identified *UNC13B* variants in individuals affected by partial epilepsies and/or febrile seizures all of whom had favourable outcome with anti-epileptic treatment without intellectual or development abnormalities, including the patients who experienced daily seizures. *Unc13b* knockdown flies resulted in seizure-like behaviour and increased neuronal firing; however, the phenotype was less severe than that of *Scn1a* knockdown flies, consistent with our clinical observations of a milder epilepsy phenotype associated with *UNC13B* variants. Thus, *UNC13B* is potentially associated with partial epilepsy. Screening for *UNC13B* variants can identify individuals who require clinical attention for possibly frequent daily seizures but can be managed with anti-epileptic therapy.

Acknowledgements

We thank the patients and their families for participating in this study. We thank Dr Li-Wu Guo for critically reading the manuscript and providing excellent suggestions; the staff at Beijing Genome Institute—ShenZhen and Chigene (Beijing) Translational Medical Research Center Co. for next-generation sequencing, analysis of genetic diseases and discussion; TsingHua Fly Center for donating transgenic RNAi lines; and Schrödinger (New York, NY, USA) for supporting open-source PyMOL software.

Funding

This work was supported by grants from the Science and Technology Project of Guangdong Province (no. 2017B030314159 to W.L.); Science and Technology Project of Guangzhou (no. 201904020028 to W.L., no. 201904010275 to Y.S., no. 20181A011076 and no.20181A011076 to J.W., and no. 201904010292 to N.H.); Multi-Center Clinical Research Fund Project of the Second Affiliated Hospital of Guangzhou Medical University (no. DZX-002 to W.L.) and Collaborative Innovation Center for Neurogenetics and Channelopathies. The funders had no role in study design, data collection and analysis and decision to publish or in manuscript preparation.

Competing interests

The authors report no competing interests.

Supplementary material

Supplementary material is available at *Brain* online.

References

1. Bhalla D, Godet B, Druet-Cabanac M, Preux PM. Etiologies of epilepsy: comprehensive review. *Expert Rev Neurother*. 2011;11(6):861–876.
2. Shorvon SD. The etiologic classification of epilepsy. *Epilepsia*. 2011;52(6):1052–1057.
3. Strug LJ, Clarke T, Chiang T, et al. Centrotemporal sharp wave EEG trait in Rolandic epilepsy maps to Elongator Protein Complex 4 (ELP4). *Eur J Hum Genet*. 2009;17(9):1171–1181.
4. Lemke JR, Lal D, Reinthaler EM, et al. Mutations in GRIN2A cause idiopathic focal epilepsy with Rolandic spikes. *Nat Genet*. 2013;45(9):1067–1072.
5. Lal D, Reinthaler EM, Schubert J, et al. DEPDC5 mutations in genetic focal epilepsies of childhood. *Ann Neurol*. 2014;75(5):788–792.
6. Michelucci R, Mecarelli O, Bovo G, et al. A *de novo* LGI1 mutation causing idiopathic partial epilepsy with telephone-induced seizures. *Neurology*. 2007;68(24):2150–2151.
7. Piton A, Redin C, Mandel JL. XLID-causing mutations and associated genes challenged in light of data from large-scale human exome sequencing. *Am J Hum Genet*. 2013;93(2):368–383.
8. Reinthaler EM, Lal D, Jurkowski W, et al. Analysis of ELP4, SRPX2, and interacting genes in typical and atypical Rolandic epilepsy. *Epilepsia*. 2014;55(8):e89–e93.
9. Kasperavičiūtė D, Catarino CB, Heinzen EL, et al. Common genetic variation and susceptibility to partial epilepsies: A genome-wide association study. *Brain*. 2010;133(7):2136–2147.
10. Wang JY, Zhou P, Wang J, et al. ARHGEF9 mutations in epileptic encephalopathy/intellectual disability: toward understanding the mechanism underlying phenotypic variation. *Neurogenetics*. 2018;19(1):9–16.
11. CONVERGE consortium. Sparse whole-genome sequencing identifies two loci for major depressive disorder. *Nature*. 2015;523(7562):588–591.
12. Shi YW, Zhang Q, Cai K, et al. Synaptic clustering differences due to different GABRB3 mutations cause variable epilepsy syndromes. *Brain*. 2019;142(10):3028–3044.
13. Cai K, Wang J, Eissman J, et al. A missense mutation in SLC6A1 associated with Lennox-Gastaut syndrome impairs GABA transporter 1 protein trafficking and function. *Exp Neurol*. 2019;320:112973.
14. Wang J, Lin ZJ, Liu L, et al. Epilepsy-associated genes. *Seizure*. 2017; 44: 11–20.
15. Ni JQ, Zhou R, Czech B, et al. A genome-scale shRNA resource for transgenic RNAi in *Drosophila*. *Nat Methods*. 2011;8(5):405–407.
16. Parker L, Howlett IC, Rusan ZM, Tanouye MA. Seizure and epilepsy: Studies of seizure disorders in *Drosophila*. *Int Rev Neurobiol*. 2011; 99: 1–21.
17. Perkins KL. Cell-attached voltage-clamp and current-clamp recording and stimulation techniques in brain slices. *J Neurosci Methods* 2006;154(1-2):1–18.
18. Gu H, O'Dowd DK. Cholinergic synaptic transmission in adult *Drosophila* Kenyon cells *in situ*. *J Neurosci*. 2006;26(1):265–272.
19. Walter AM, Böhme MA, Sigrist SJ. Vesicle release site organization at synaptic active zones. *Neurosci Res*. 2018;127:3–13.

20. Parker L, Padilla M, Du Y, Dong K, Tanouye MA. *Drosophila* as a model for epilepsy: BSS is a gain-of-function mutation in the para sodium channel gene that leads to seizures. *Genetics*. 2011; 187:523–534.
21. Olsen SR, Bhandawat V, Wilson RI. Excitatory interactions between olfactory processing channels in the *Drosophila* antennal lobe. *Neuron* 2007;54(1):89–103.
22. Pinheiro PS, Houy S, Sørensen JB. C2-domain containing calcium sensors in neuroendocrine secretion. *J Neurochem*. 2016; 139(6):943–958.
23. Dittman JS. Unc13: A multifunctional synaptic marvel. *Curr Opin Neurobiol*. 2019;57:17–25.
24. He E, Wierda K, van Westen R, et al. Munc13-1 and Munc18-1 together prevent NSF-dependent de-priming of synaptic vesicles. *Nat Commun*. 2017;8:15915.
25. Gioia DA, Alexander NJ, McCool BA. Differential expression of Munc13-2 produces unique synaptic phenotypes in the basolateral amygdala of C57BL/6J and DBA/2J mice. *J Neurosci*. 2016; 36(43):10964–10977.
26. Rodríguez-Castañeda F, Maestre-Martínez M, Coudevylle N, et al. Modular architecture of Munc13/calmodulin complexes: dual regulation by Ca^{2+} and possible function in short-term synaptic plasticity. *EMBO J*. 2010;29(3):680–691.
27. Shin OH, Lu J, Rhee JS, et al. Munc13 C2B domain is an activity-dependent Ca^{2+} regulator of synaptic exocytosis. *Nat Struct Mol Biol*. 2010;17(3):280–288.
28. Michelassi F, Liu H, Hu Z, Dittman JS. A C1-C2 module in Munc13 inhibits calcium-dependent neurotransmitter release. *Neuron*. 2017;95(3):577–590.
29. Lipstein N, Verhoeven-Duif NM, Michelassi FE, et al. Synaptic UNC13A protein variant causes increased neurotransmission and dyskinetic movement disorder. *J Clin Invest*. 2017; 127 (3): 1005–18.
30. Varoqueaux F, Sigler A, Rhee JS, et al. Total arrest of spontaneous and evoked synaptic transmission but normal synaptogenesis in the absence of Munc13-mediated vesicle priming. *Proc Natl Acad Sci U S A*. 2002;99(13):9037–9042.
31. Lammertse HCA, van Berkel AA, Iacomino M, et al. Homozygous STXBP1 variant causes encephalopathy and gain-of-function in synaptic transmission. *Brain*. 2020;143(2):441–451.
32. Kovacevic J, Maroteaux G, Schut D, et al. Protein instability, haploinsufficiency, and cortical hyper-excitability underlie STXBP1 encephalopathy. *Brain*. 2018;141(5):1350–1374.
33. Wei F, Yan LM, Su T, et al. Ion channel genes and epilepsy: Functional alteration, pathogenic potential, and mechanism of epilepsy. *Neurosci Bull*. 2017;33(4):455–477.
34. Jiang X, Raju PK, D'Avanzo N, et al. Both gain-of-function and loss-of-function *de novo* CACNA1A mutations cause severe developmental epileptic encephalopathies in the spectrum of Lennox-Gastaut syndrome. *Epilepsia*. 2019;60(9):1881–1894.
35. He N, Lin ZJ, Wang J, et al. Evaluating the pathogenic potential of genes with *de novo* variants in epileptic encephalopathies. *Genet Med*. 2019;21(1):17–27.
36. Augustin I, Betz A, Herrmann C, Jo T, Brose N. Differential expression of two novel Munc13 proteins in rat brain. *Biochem J*. 1999;337(3):363–371.
37. Meng H, Xu HQ, Yu L, et al. The SCN1A mutation database: Updating information and analysis of the relationships among genotype, functional alteration, and phenotype. *Hum Mutat*. 2015;36(6):573–580.
38. Tang B, Li B, Gao LD, et al. Optimization of *in silico* tools for predicting genetic variants: Individualizing for genes with molecular sub-regional stratification. *Brief Bioinform*. 2020;21(5): 1776–1786.
39. Bi C, Wu J, Jiang T, et al. Mutations of ANK3 identified by exome sequencing are associated with autism susceptibility. *Hum Mutat*. 2012;33(12):1635–1638.
40. Kataoka M, Matoba N, Sawada T, et al. Exome sequencing for bipolar disorder points to roles of *de novo* loss-of-function and protein-altering mutations. *Mol Psychiatry*. 2016;21(7):885–893.
41. Nakamura T, Jimbo K, Nakajima K, Tsuboi T, Kato T. *De novo* UNC13B mutation identified in a bipolar disorder patient increases a rare exon-skipping variant. *Neuropsychopharmacol Rep*. 2018;38(4):210–213.